Single surface phaseless characterization of antennas via hierarchically-ordered optimizations

Single-Surface Phaseless Characterization of Antennas via Hierarchically-Ordered Optimizations

A. F. Morabito, R. Palmeri, V. A. Morabito, A. R. Laganà, and T. Isernia

***Abstract*—A new approach for determining the complex scalar field radiated by a finite-dimensional source starting from its modulus is proposed and assessed. First, by introducing a suitable relaxation, we show that the original problem can be conveniently tackled in terms of a finite number of different Convex Programming problems. Then, an effective procedure for dealing with a small number of hierarchically-ordered optimizations is introduced and discussed. Numerical experiments, including consideration of an actual radiating source and of noisy data, are provided with reference to the canonical case of far-field data and array antennas.**

***Index Terms*—Antenna measurements, antenna pattern synthesis, phase retrieval.**

I. Introduction

The Phase Retrieval (PR) problem is of high interest in very many fields where the full knowledge of a complex function is needed but phase measurements are not available or not convenient. These scenarios include (but are not limited to) astronomy [1], crystallography [2], lithography [3], and electronic microscopy [4],[5].

The problem has been the object of very many studies also in the Antennas & Propagation community (see for instance [6]-[26]) because of its interest in antenna characterization (including near-field [13] or far-field [14] phaseless measurements) and in the synthesis of power-pattern nominal distributions. PR is also of interest in applications regarding radio telescopes [12] and inverse-scattering-based imaging [27]. Moreover, since phase measurements require a precise positioning which is not always available in UAV and high-frequency applications, it plays an important role in the THz regime [17] and antenna testing through UAV [28]. Finally, the possible electromagnetic applications of PR at radio or microwave frequency include the magnetic-resonance-based electrical properties tomography [29].

If $f(\underline{x})$ is an unknown signal and T is an operator such that $F(\underline{u})=T[f(\underline{x})]=|F(\underline{u})|e^{j\varphi(\underline{u})}$ ($\underline{x}$ and $\underline{u}$ denoting the vectors spanning the corresponding multidimensional domains), a very wide class of PR problems can be formulated as follows:

Determine $f(\underline{x})$ from $|F(\underline{u})|$ and some additional a-priori information.

Notably, the above formulation concerns both continuous and discrete signals, and the a-priori information may include the knowledge of the support of $f(\underline{x})$, or of its being positive, or other kinds of partial knowledge of $f(\underline{x})$.

A large attention has been devoted in the literature to the case where T is a *Fourier* transform operator. In this case, which is the one we will deal with in the remainder of the paper, PR is also strictly related to the synthesis of a given power pattern by means of linear or planar sources. In particular, we will deal in the following with the case of discrete sources, i.e., array antennas. Notably, as the far field of any non-superdirective source can be processed, in the visible part of the spectrum, as it is radiated by a 'virtual' equispaced array (see for instance [30]-[33]), results which follow have a range of validity which is not restricted to discrete and equispaced sources.

As a distinguishing characteristic, differently from (essentially all) the approaches available in the literature which require two different sets of measurements in order to have a reliable retrieval procedure (two near-field surfaces in [7]-[9],[11],[13],[18], two different defocus conditions in [3],[4], two different probes in [15],[16]), we propose in the following a method which just requires *a single* set of measurement (plus some minimum a-priori information or a minimal number of additional measurements regarding single points rather than a whole plane or the like).

Also note that while the approach is presented (for the sake of simplicity) for the case of far-field measurements, it can be applied to near-field measurements in a very simple fashion.

In the following, Section II recalls some basic theoretical and methodological results in PR. Then, in Sections III, IV, and V, the proposed solution procedures are respectively presented, improved, and assessed. Conclusions follow.

II. Some basic result in phase retrieval

Effective solution of PR requires addressing a number of theoretical and operative issues which are intrinsic to the

This is the post-print of the following article: A. F. Morabito, R. Palmeri, V. A. Morabito, A. R. Laganà, and T. Isernia, "Single-Surface Phaseless Characterization of Antennas via Hierarchically Ordered Optimizations," IEEE Transactions on Antennas and Propagation, vol. 67, n. 1, pp. 461-474, 2019. Article has been published in final form at: https://ieeexplore.ieee.org/document/8502061. DOI: 10.1109/TAP.2018.2877270.

problem itself. In order to highlight the potentialities of the new approach we are going to present, these issues (along with some of the corresponding way outs) are recalled in the following.

A first important issue is of course concerned with *uniqueness* (or *non-uniqueness*) of the solution of the problem. In this regard, it is well known that in both 1-D and 2-D cases PR of band-limited signals[1] is affected by the so-called 'trivial ambiguities' [34], i.e., modifications of $f(\underline{x})$ which all lead to the same $|F(\underline{u})|$ distribution. These latter can either be a constant phase, or a translation of f [leading to a linear phase on F], or a reversal along $\underline{x}$ plus complex conjugation of f [leading to a conjugation of F], or any combination of them. However, while conjugate solutions can be avoided only by exploiting some *a-priori* information on f or F, the ambiguities related to a constant phase can be removed by fixing the phase of F at a given point once and for all, while the ones related to a linear phase can be removed by knowing the f support (provided f is not equal to zero all over its border) [34],[35].

Other than by trivial ambiguities, if T is a Fourier-transform operator, non-uniqueness of the solution can also be induced by the fact that $|F|^2$ can be written as a trigonometric polynomial which can be reduced to a product of first-order factors where 'zero flipping' generates multiple phase solutions [36]. This issue does not affect the 2-D case but for a *zero measure* set of instances wherein 2-D polynomials are factorable [35]. On the other side, such a zero measure set of cases includes 'u-v factorable' and circularly-symmetric F distributions. In all these instances, however, some additional a-priori information (such as a single or a few samples of f as well as a single or a few amplitude and phase measurements of F) allows fixing ambiguities and restoring theoretical uniqueness.

However, this is not the end of the story, as a second difficulty, namely the *non-linearity* of the problem, comes into play. In fact, even if the available information allows theoretically ensuring the uniqueness of the solution, the non-linearity of the problem may still result in a retrieved signal which is actually different from the ground truth. In fact, while procedures based on a local optimization of a cost function may get trapped into 'false' solutions [37], the computational burden of global-optimization techniques exponentially grows with the number of unknowns [38], so that they can still fail in the limited time one has at disposal. This is one of the main reasons for the exploitation of two different sets of measurements in essentially all of the existing literature (see above).

Very many different procedures have been proposed to solve PR problems. A rather popular approach (using two different sets of measures) is given by the so-called alternating projections onto (non-convex) sets [39]. However, this technique is equivalent to a local optimization, and hence it is prone to false solutions. As a variant of the basic alternating projections approach, the Hybrid Input-Output (HIO) algorithm has been proposed by Fienup in [40]. However, while being known as relatively-robust to false solutions, HIO does not guarantee convergence to the ground truth. Some insight into the false-solutions problem and effective procedures have been also possible by formulating PR as a quadratic inverse problem [41]. Recently, an approach has also been discussed in [42] where PR is reduced to a linear problem by introducing a large number of auxiliary variables and a relaxation of the original problem. However, the number of introduced auxiliary variables quadratically grows with the number of actual unknowns. Such a circumstance, along with the relaxation of the original non-convex problem into a convex one, implies that the false-solutions problem is still an open issue.

A third and final set of difficulties, which is indeed specific of antenna applications, concerns the actual availability of $|F(\underline{u})|$ measurements. In fact, differently from a generic PR problem wherein measurements can be taken over the whole domain of the function, in antenna applications measuring will be possible just over the *visible* range. By way of illustration, this circumstance is represented in Fig. 1 with reference to equispaced array antennas and far-field measurements: as graphically recalled, the signal domain is not always fully available to the measurement system. Further details and comments on this issue are given in Appendix I.

Due to the above limitations, it makes sense to look for and eventually introduce different points of view allowing some additional understanding of the difficulties related to the non-linearity of the PR problem, as well as to devise new effective solution strategies. This was also the spirit of [43], wherein we introduced a technique for solving a wide class of problems by means of a 'tunneling' strategy which allows escaping from false solutions.

In this paper, by further developing the 'power inflation' strategy introduced in [43], we present a new approach allowing to relax PR into a combination of Convex Programming (CP) problems and propose an innovative strategy to avoid false solutions. By taking advantage of such a setting, a further effective solution procedure approaching PR as a minimum number of hierarchically-ordered optimizations is introduced and discussed, and antenna applications are given and tested.

[1] Fourier transform of signals having a finite support.

This is the post-print of the following article: A. F. Morabito, R. Palmeri, V. A. Morabito, A. R. Laganà, and T. Isernia, "Single-Surface Phaseless Characterization of Antennas via Hierarchically Ordered Optimizations," IEEE Transactions on Antennas and Propagation, vol. 67, n. 1, pp. 461-474, 2019. Article has been published in final form at: https://ieeexplore.ieee.org/document/8502061. DOI: 10.1109/TAP.2018.2877270.

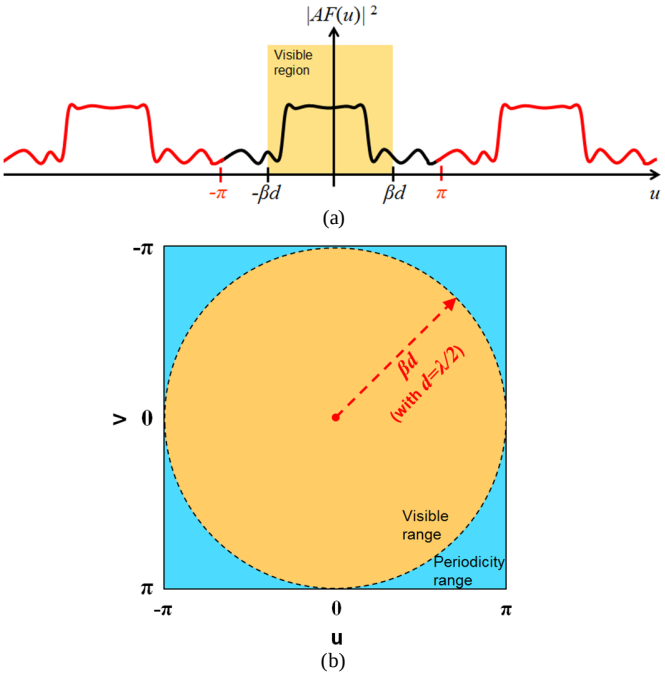

Fig. 1. Comparison between *periodicity* and *visible* ranges for power-pattern antenna measurements: (a) linear equispaced arrays; (b) planar equispaced arrays on a square grid [*AF*, λ, β, d, u, and v respectively denoting the array factor, the wavelength, the wavenumber, the inter-element distance along both x and y axes, and the spectral variables (see also Section III and Appendix I)].

III. Phase Retrieval as a Combination of CP Problems

For the sake of simplicity, we present in the following the proposed approach in the 1-D case (while the numerical assessment in Section V will also include 2-D experiments).

Denoting by d and θ the inter-element spacing and the angle between the array axis and the observation direction, the far field radiated by a one-dimensional array composed of N isotropic antennas is given by:

$$AF(u)=\sum_{n=0}^{N-1} I_n e^{jnu} \qquad (1)$$

wherein $u=\beta d\cos\theta$ ($\beta=2\pi/\lambda$ being the wavenumber, with the λ wavelength) and the sequence $I_0,\ldots,I_{N-1}$ denotes the elements' complex excitations. Then, by setting *AF* as the *F* function described in Section I[2], and by denoting by M^2 the measured square-amplitude far-field distribution, PR amounts to find $I_0,\ldots,I_{N-1}$ in such a way that:

$$\left|\sum_{n=0}^{N-1} I_n e^{jnu}\right|^2 = M^2(u) \qquad (2)$$

and no additional constraint or information is used in a first instance.

Then, a very general PR formulation (see also [43]) can be given as:

Find the sequence $I_0,\ldots,I_{N-1}$ such that:

$$\max_{I_o,\ \ldots,\ I_{N-1}} \sum_{k=1}^{K} |AF(u_k)|^2 \qquad (3.a)$$

subject to:

$$|AF(u_k)|^2 \le M^2(u_k) \qquad k=1,\ldots,K' \qquad (3.b)$$

and to some additional constraint guaranteeing the theoretical uniqueness of a solution.

In (3.a)-(3.b), which will be referred in the following as *problem 1*, $u_1,\ldots,u_K$ denotes a sufficiently fine discretization. In particular, due to bandlimitedness of radiated fields [44], $K=2N$ uniformly-spaced samples of $|AF(u)|^2$ are considered in (3.a), while some additional sample is needed in (3.b) in order to enforce that the tentative square amplitude distribution is everywhere below or equal to the square amplitude data [45].

Obviously, the final goal is that the tentative square-amplitude distribution collapses onto the measured one. In fact, *problem 1* can be interpreted as an 'inflation' of the function $|AF(u)|^2$ until it reaches the ground truth.

Notably, constraints (3.b) define a convex set [46] and, in the actual case where measurements are affected by noise, they can be modified into:

$$|AF(u_k)|^2 \le M^2(u_k)+\varepsilon_1 \qquad k=1,\ldots,K' \qquad (3.c)$$

(where ε_1 is related to the estimated noise) which are still convex.

However, because of the form of (3.a), *problem 1* amounts to *maximize* a positive-definite quadratic function in a convex set. As such, it belongs to the class of NP-hard problems, with the inherent computational difficulties [47]. In particular, it is prone to the possible occurrence of local optima where the procedure may get trapped, which correspond to the usual false solutions issue experienced by other PR approaches [37]. In this respect, a possible way out is given by the following procedure:

1. partition the overall search space in such a way that each sub-region contains *only one* possible solution;
2. solve the optimization problem in each sub-region;
3. pick the actual solution (amongst all the results coming out from step 2) by using some additional information, e.g., a single or a few known excitations, or a single or a few amplitude-and-phase measurements.

[2] We stress that such a setting gives to the proposed approach a very large application range. In fact, expansion (1) can be used to express the far field of a variety of radiating systems, including continuous aperture sources (through the technique in [31] and arrays with whatever element patterns and locations where mutual-coupling and mounting-platform effects are also present (through the method in [32]). Finally, by exploiting the 'reduced radiated field' concept introduced in [33], expansion (1) can also be used to express the near-field distribution associated to a given source.

This is the post-print of the following article: A. F. Morabito, R. Palmeri, V. A. Morabito, A. R. Laganà, and T. Isernia, "Single-Surface Phaseless Characterization of Antennas via Hierarchically Ordered Optimizations," IEEE Transactions on Antennas and Propagation, vol. 67, n. 1, pp. 461-474, 2019. Article has been published in final form at: https://ieeexplore.ieee.org/document/8502061. DOI: 10.1109/TAP.2018.2877270.

Unfortunately, we were not able to perform such a partition for functional (3.a). However, an effective strategy allowing such a splitting is that of modifying the objective function of *problem 1* by changing the goal into:

$$\max_{I_0,\ \ldots,\ I_{N-1}} \sum_{k=1}^{K''} \left\{ \left| \mathrm{Re}\left[AF(u_k)\right] \right| + \left| \mathrm{Im}\left[AF(u_k)\right] \right| \right\} \qquad (3.d)$$

wherein, since the array factor is a bandlimited function requiring N samples, we assume from now on $K''=N$. Saying it in other words, we relax the original ℓ_2-norm optimization (3.a) into the ℓ_1-norm optimization (3.d). Such a relaxation follows somehow (from a different perspective) a recent trend in the Signal Processing and Antennas & Propagation communities, where a number of relaxations (the one from the ℓ_0 to ℓ_1 norms inherent in Compressive Sensing [48], as well as the ones respectively inherent in the Semidefinite Relaxation technique [49] and in the Matrix Completion method [50]) have been fruitfully introduced.

Advantages of the proposed relaxation are as follows.

The maximization problem (3.d) subject to constraints (3.b), which will be referred in the following as *problem 2*, can be written as a CP problem in any subspace defined by the intersection of the following constraints:

$$\begin{cases} \mathrm{Re}\left[AF\left(u_1\right)\right] \le 0 \quad or \quad \mathrm{Re}\left[AF\left(u_1\right)\right] \ge 0 \\ \mathrm{Im}\left[AF\left(u_1\right)\right] \le 0 \quad or \quad \mathrm{Im}\left[AF\left(u_1\right)\right] \ge 0 \\ \mathrm{Re}\left[AF\left(u_2\right)\right] \le 0 \quad or \quad \mathrm{Re}\left[AF\left(u_2\right)\right] \ge 0 \\ \mathrm{Im}\left[AF\left(u_2\right)\right] \le 0 \quad or \quad \mathrm{Im}\left[AF\left(u_2\right)\right] \ge 0 \\ \ldots \\ \mathrm{Re}\left[AF\left(u_{K''}\right)\right] \le 0 \quad or \quad \mathrm{Re}\left[AF\left(u_{K''}\right)\right] \ge 0 \\ \mathrm{Im}\left[AF\left(u_{K''}\right)\right] \le 0 \quad or \quad \mathrm{Im}\left[AF\left(u_{K''}\right)\right] \ge 0 \end{cases} \qquad (4)$$

In fact, any of these intersections represents a 'hyper quadrant' in the space $\{\mathrm{Re}[AF(u_1)],\mathrm{Im}[AF(u_1)],\ldots, \mathrm{Re}[AF(u_N)],\mathrm{Im}[AF(u_N)]\}$. Moreover, by means of a proper choice of the signs of the real and imaginary parts of the field, the cost function (3.d) can be rewritten as the minimization of a *linear* function of the real and imaginary parts of $AF(u_1),\ldots,AF(u_{K''})$. For example, in the first hyper quadrant, i.e., $\{\mathrm{Re}[AF(u_k)]\ge 0,\mathrm{Im}[AF(u_k)]\ge 0\}$, $k=1,\ldots,K''$, the optimization problem becomes:

$$\min_{I_0,\ \ldots,\ I_{N-1}} -\sum_{k=1}^{K''} \left\{ \mathrm{Re}\left[AF\left(u_k\right)\right] + \mathrm{Im}\left[AF\left(u_k\right)\right] \right\} \qquad (5)$$

A number of comments are now in order on *problem 2*.

First, it is worth noting that PR has been turned into a combinatorial problem where one looks for the right combination of signs of both the real and imaginary parts of $AF(u_k)$, $k=1,\ldots,K''$. In fact, in each hyper quadrant, *problem 2* belongs to the CP class, which entails that a *single* (and hence globally-optimal) solution exists for each of the instances in (4).

Second, we stress that the approach can be safely used also in those cases where the unknown signal cannot be turned into 1-D polynomials and hence the problem cannot be solved according to the procedure in [36].

On the other side, the new formulation has two drawbacks:

a) as pictorially represented in Fig. 2, in each hyper quadrant the maximum of the cost function of *problem 2* does not always correspond to the maximum of the cost function of *problem 1*;

b) consideration of all possible hyper quadrants results in a rapid growth of the number P of CP problems, which raises as $P=2^{2K''}$.

As far as point (a) is concerned, in a large set of experiments (dealing with both linear and planar arrays – see Section V) we experienced that the solution of *problem 2* tends to be an excellent starting point for achieving the solution of *problem 1*. Solutions of the two problems were indeed coincident in many cases. This circumstance is related to the fact that the additional information needed in order to get a theoretically-unique solution is such that the admissible set of values is a zero-measure set in the space $\{\mathrm{Re}[AF(u_1)],\mathrm{Im}[AF(u_1)],\ldots,\mathrm{Re}[AF(u_{K''})],\mathrm{Im}[AF(u_{K''})]\}$.

As far as point (b) is concerned, a first obvious strategy amounts to reduce as much as possible the number of CP problems to be actually considered. In this respect, it proves useful to exploit the available information on the location of zeroes (or nearly-zero values) in the data. In fact, if $|AF(u_k)|^2=0$ then the four different possibilities for $\{\mathrm{Re}[AF(u_k)],\mathrm{Im}[AF(u_k)]\}$ degenerate in the single constraint $AF(u_k)=0$. Therefore, if $|AF(u)|^2$ is equal to zero in δ of the K'' sampling points then the number of CP problems to be actually solved reduces to $P=2^{2K''}/4^{\delta}=4^{K''-\delta}$.

A second strategy amounts then to reduce as much as possible the number of 'feasible' CP problems, i.e., the number of CP problems such that the intersection of the different constraints is not void. In fact, such a circumstance will avoid entering into an actual optimization, thus saving resources. In this respect, it proves useful exploiting all the available a-priori information about the ground truth which is available on $AF(u)$ or $I_0,\ldots,I_{N-1}$. Moreover, it is worth noting that any constraint of the kind:

$$\left|AF\left(u_k\right)\right|^2 \ge M^2\left(u_k\right) - \varepsilon_2 \qquad (6)$$

can be relaxed into:

$$\left|\mathrm{Re}\left[AF(u_k)\right]\right| + \left|\mathrm{Im}\left[AF(u_k)\right]\right| \ge M(u_k) - \varepsilon_3 \qquad (7)$$

where ε_2 (which is determined from the measurement accuracy) and ε_3 are small positive constants. In fact, this constraint is convex (and actually linear) in any of the

This is the post-print of the following article: A. F. Morabito, R. Palmeri, V. A. Morabito, A. R. Laganà, and T. Isernia, "Single-Surface Phaseless Characterization of Antennas via Hierarchically Ordered Optimizations," IEEE Transactions on Antennas and Propagation, vol. 67, n. 1, pp. 461-474, 2019. Article has been published in final form at: https://ieeexplore.ieee.org/document/8502061. DOI: 10.1109/TAP.2018.2877270.

subspaces corresponding to the four different possibilities for the signs of {Re[$AF(u_k)$],Im[$AF(u_k)$]} (see Fig. 3 for a better understanding). Note such a strategy also reduces the possibilities to get into the (undesired) situation depicted in Fig. 2(c).

As a third strategy, let us note that the CP problems are independent each from the other, so that advantage can be eventually taken from parallel computing.

Finally, it is worth noting that the choice of the most convenient signs for {Re[$AF(u_k)$],Im[$AF(u_k)$]} can also be tackled as the optimization of a binary string, for which effective global-optimization procedures do exist [51].

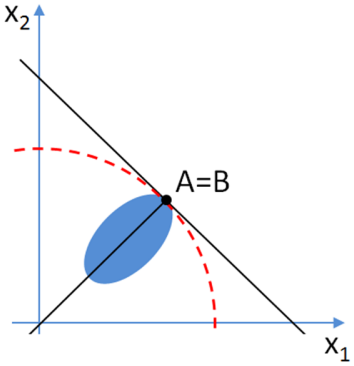

(a)

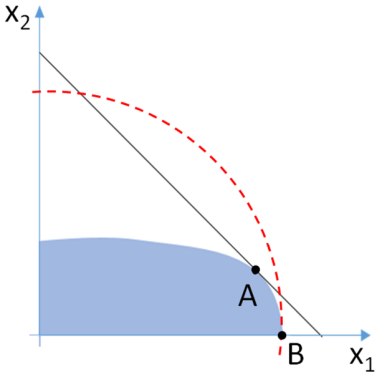

(b)

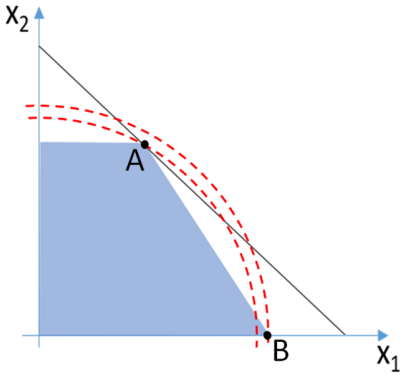

(c)

Fig. 2. Pictorial comparison of the results achievable through the maximization (in the light-blue convex set) of the functionals ($|x_1|+|x_2|$) (point *A*) and ($x_1^2+x_2^2$) (point *B*): coincident maxima (a); non-coincident maxima, *A* being an excellent starting point to achieve *B* (b); non-coincident maxima, *A* being a local maximum of ($x_1^2+x_2^2$) (c).

IV. Hierarchically-ordered optimizations for phase retrieval

A further possibility to solve *problem 1* arises from the fact that, in many cases, the maximum of either *problem 1* or *problem 2* will lie on the boundary of the corresponding hyper quadrant. In fact (see Fig. 4), the optimization procedure will often tend towards a different hyper quadrant. By taking into account such a circumstance, and the fact that data samples having a larger intensity will have a major impact on the value of the cost functions (3.a) and (3.d), a more effective way to explore the tree of all possible alternatives can be devised. In particular, one can avoid considering all the possible sign combinations, and can instead tackle the PR problem by means of the following procedure:

(i) solve *problem 2*;

(ii) if data fitting is not satisfactory, then solve *problem 1* by exploiting the solution of step (i) as the starting point;

(iii) if data fitting is not satisfactory, then repeat steps (i) and (ii) in each of the four convex sets defined by:

$$\begin{cases} \mathrm{Re}\left[AF\left(u_{MAX}\right)\right] \geq 0 \\ \mathrm{Im}\left[AF\left(u_{MAX}\right)\right] \geq 0 \end{cases} \tag{8.a}$$

or

$$\begin{cases} \mathrm{Re}\left[AF\left(u_{MAX}\right)\right] \geq 0 \\ \mathrm{Im}\left[AF\left(u_{MAX}\right)\right] \leq 0 \end{cases} \tag{8.b}$$

or

$$\begin{cases} \mathrm{Re}\left[AF\left(u_{MAX}\right)\right] \leq 0 \\ \mathrm{Im}\left[AF\left(u_{MAX}\right)\right] \geq 0 \end{cases} \tag{8.c}$$

or

This is the post-print of the following article: A. F. Morabito, R. Palmeri, V. A. Morabito, A. R. Laganà, and T. Isernia, "Single-Surface Phaseless Characterization of Antennas via Hierarchically Ordered Optimizations," IEEE Transactions on Antennas and Propagation, vol. 67, n. 1, pp. 461-474, 2019. Article has been published in final form at: https://ieeexplore.ieee.org/document/8502061. DOI: 10.1109/TAP.2018.2877270.

$$\begin{cases} \mathrm{Re}\left[AF\left(u_{MAX}\right)\right] \le 0 \\ \mathrm{Im}\left[AF\left(u_{MAX}\right)\right] \le 0 \end{cases} \quad (8.d)$$

where u_{MAX} is the sampling point corresponding to the largest $|AF(u)|$ value;

(iv) if data fitting is not satisfactory, then repeat steps (i) and (ii) in each of the sixteen sets determined by the intersection of each of constraints (8) with each of the following constraints:

$$\begin{cases} \mathrm{Re}\left[AF\left(u_{II}\right)\right] \ge 0 \\ \mathrm{Im}\left[AF\left(u_{II}\right)\right] \ge 0 \end{cases} \quad (9.a)$$

or

$$\begin{cases} \mathrm{Re}\left[AF\left(u_{II}\right)\right] \ge 0 \\ \mathrm{Im}\left[AF\left(u_{II}\right)\right] \le 0 \end{cases} \quad (9.b)$$

or

$$\begin{cases} \mathrm{Re}\left[AF\left(u_{II}\right)\right] \le 0 \\ \mathrm{Im}\left[AF\left(u_{II}\right)\right] \ge 0 \end{cases} \quad (9.c)$$

or

$$\begin{cases} \mathrm{Re}\left[AF\left(u_{II}\right)\right] \le 0 \\ \mathrm{Im}\left[AF\left(u_{II}\right)\right] \le 0 \end{cases} \quad (9.d)$$

where u_{II} is the sampling point corresponding to the second largest $|AF(u)|$ value;

(v) if data fitting is not satisfactory, then iterate the procedure by enforcing constraints relative to data samples having a smaller and smaller intensity until a fully-satisfactory fitting between the solution and the ground truth is achieved.

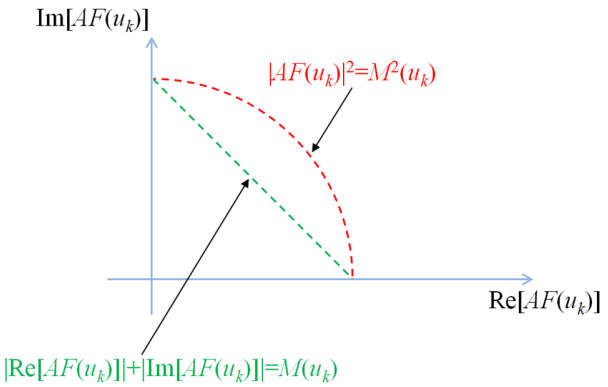

Fig. 3. Pictorial comparison between the curves involved in the relaxation of (6) into (7).

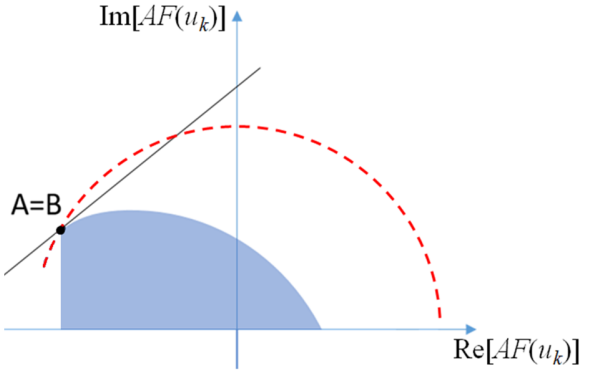

Fig. 4. Pictorial representation of a case wherein the solutions of *problem 1* and *problem 2* tend to escape from the first hyper quadrant.

In the worst case the procedure will still need to explore all the 2^{2K} hyper quadrants. However, it is expected that the consideration of a few larger subspaces will allow a satisfactory data fitting, thus leading to the retrieval of the actual ground truth. This expectation has been confirmed by a large number of numerical examples (a part of which is reported in the next Section).

Notably, all the presented solution procedures can be applied to generic sources provided that (1) is replaced with the actual field distribution over a given surface. For instance, if the source is an equispaced planar array lying on the *x*-*y* plane and composed, according to a rectangular grid, by Q elements along x (with a spacing equal to d_x) and S elements along y (with a spacing equal to d_y), then it will be:

$$AF(u,v) = \sum_{q=0}^{Q-1}\sum_{s=0}^{S-1} I_{q,s} e^{j(qu+sv)} \quad (10)$$

wherein $u=\beta d_x \sin\alpha\cos\varphi$ and $v=\beta d_y \sin\alpha\sin\varphi$ (α and φ being the aperture elevation and azimuth angles, respectively) while $I_{q,s}$ denotes the excitation of the element located on the intersection between the s-th row and the q-th column of the array layout. In this case, in order to have a number of independent data not smaller than the number of unknowns, a lower bound on the inter-element spacing as detailed in Appendix I has to be fulfilled.

V. Numerical Assessment

Several numerical experiments have been performed in order to assess the proposed approach in both cases of 1-D and 2-D sources.

The square-amplitude field measurements have been simulated under the hypothesis of far-field data and, in order to make the PR scenario as realistic as possible, each sample has been corrupted by an additive white Gaussian noise such to realize a given value of Signal to Noise Ratio (SNR). Therefore, a smooth scaling of the upper-bound function in

This is the post-print of the following article: A. F. Morabito, R. Palmeri, V. A. Morabito, A. R. Laganà, and T. Isernia, "Single-Surface Phaseless Characterization of Antennas via Hierarchically Ordered Optimizations," IEEE Transactions on Antennas and Propagation, vol. 67, n. 1, pp. 461-474, 2019. Article has been published in final form at: https://ieeexplore.ieee.org/document/8502061. DOI: 10.1109/TAP.2018.2877270.

(3.b) has been used in such a way that the actual square-amplitude distribution can be safely allocated within the upper mask.

In order to counteract the occurrence of trivial ambiguities and other kinds of non-uniqueness, in all experiments the support of the source and one excitation have been assumed a-priori known.

The numerical tool adopted to solve the different problems is the local-optimization 'fmincon' routine of Matlab™, whose starting point has been chosen in step (i) as excitations equal to zero over the whole array aperture. By exploiting a calculator having an Intel Core i7-3537U 2.50GHz CPU and a 10 GB RAM, the solution of every single optimization required less than 10 seconds in all 1-D examples and less than 1 minute in all 2-D cases (but for the final experiment dealing with a 100-elements planar array).

In order to perform a quantitative assessment, according to the common habit in PR problems (see for instance [52]), in each test case we evaluated the Normalized Mean Square Error (NMSE), i.e.:

$$NMSE = \frac{\left\| \underline{I}_{ref} - \underline{I}_{retrieved} \right\|^2}{\left\| \underline{I}_{ref} \right\|^2} \qquad (11)$$

wherein $\underline{I}_{ref}$ and $\underline{I}_{retrieved}$ denote the vectors containing the true and retrieved excitations, respectively. Then, we considered 'satisfactory' the retrieved sources allowing NMSE<10^{-1}.

In the following, the outcomes achieved in the cases of 1-D and 2-D sources are separately described in Subsections V.A and V.B, respectively.

V.A One-dimensional arrays

In order to assess the proposed approach in 1-D problems, we present in the following the outcomes achieved by exploiting as reference some 'popular' fields adopted in benchmarking synthesis procedures which are relative to isotropic element patterns as well as a 'realistic' field generated through full-wave simulations. Notably, the latter takes into account the actual element patterns as well as mutual-coupling and mounting-platform effects. All experiments have been performed by setting SNR=25 dB.

In the first test case, we considered as radiating source the array synthesized in [53], which is composed by N=16 isotropic elements (with a $d=\lambda/2$ constant spacing) and generate, under the excitations depicted in blue color in Fig. 5, the square-cosecant power pattern [53],[54] shown in blue color in Fig. 6.

Execution of step (i) of the procedure led to the excitations depicted in red color in Fig. 5 (NMSE=0.3006). The corresponding power pattern is shown in green color in Fig. 6. As it can be seen, the fitting between data and solutions did not result fully satisfactory. Therefore, step (ii) of the procedure has also been executed. By so doing, a much better fitting (i.e., NMSE=0.0024) has been achieved. The excitations retrieved through step (ii) and the corresponding power pattern are depicted in red color in figures 7 and 6, respectively.

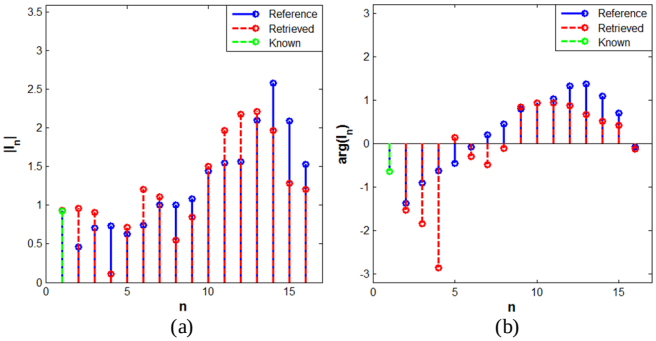

Fig. 5. Excitation amplitudes (a) and phases (b) concerning the retrieval of the source synthesized in [53]: comparison between the ground truth (blue curve) and the solution achieved by performing **only step (i)** of the proposed procedure (red curve). The a-priori known excitation is plotted in green color.

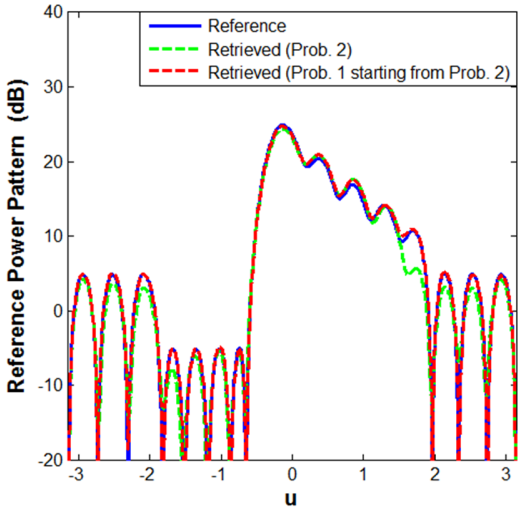

Fig. 6. Power patterns corresponding to PR of the source designed in [53]: ground truth (blue curve); solution achieved by performing **only step (i)** of the proposed procedure (green curve); solution achieved by performing **steps (i) and (ii)** of the proposed procedure (red curve). SNR=25 dB.

This is the post-print of the following article: A. F. Morabito, R. Palmeri, V. A. Morabito, A. R. Laganà, and T. Isernia, "Single-Surface Phaseless Characterization of Antennas via Hierarchically Ordered Optimizations," IEEE Transactions on Antennas and Propagation, vol. 67, n. 1, pp. 461-474, 2019. Article has been published in final form at: https://ieeexplore.ieee.org/document/8502061. DOI: 10.1109/TAP.2018.2877270.

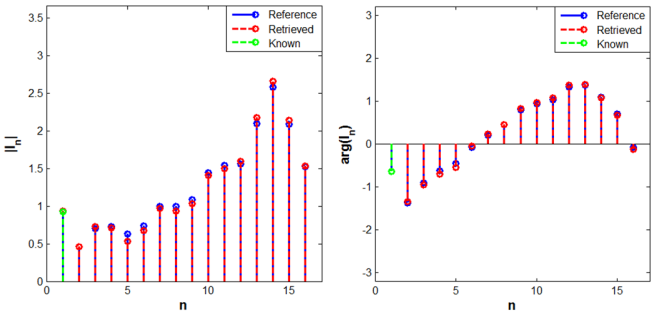

Fig. 7. Excitation amplitudes (a) and phases (b) concerning the retrieval of the source synthesized in [53]: comparison between the ground truth (blue curve) and the solution achieved by performing **steps (i) and (ii)** of the proposed procedure (red curve). The a-priori known excitation is plotted in green color.

In the second test case, we set as signal source the array designed in [36]. The latter, which is composed of N=15 isotropic elements with a $d=\lambda/2$ constant spacing, generates (under the excitations shown in blue color in Fig. 8) the flat-top power pattern depicted in Fig. 9.

By executing step (i) of the procedure, the excitations depicted in red color in Fig. 8 and the power pattern depicted in green color in Fig. 9 have been achieved. As it can be seen, the fitting between data and solutions did not result fully satisfactory (i.e., NMSE=1.6102). Therefore, step (ii) of the procedure has been also executed. By so doing, the excitations shown in Fig. 10 have been achieved. The corresponding power pattern is depicted in red color in Fig. 9. As it can be seen, execution of step (ii) of the procedure allowed a fully satisfactory (i.e., NMSE=0.0021) fitting between data and solution.

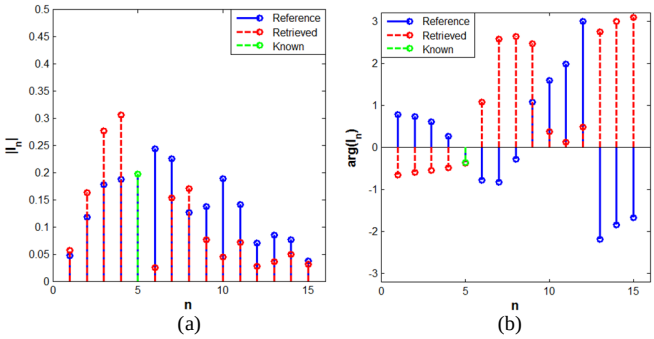

Fig. 8. Excitation amplitudes (a) and phases (b) concerning the retrieval of the source synthesized in [36]: comparison between the ground truth (blue curve) and the solution achieved by performing **step (i)** of the proposed procedure (red curve). The a-priori known excitation is depicted in green color.

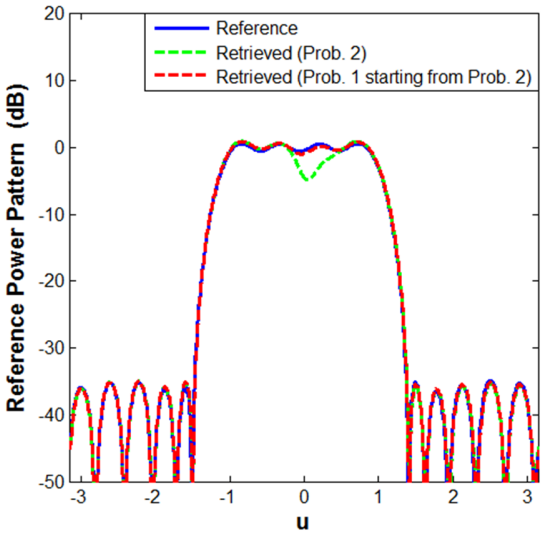

Fig. 9. Power patterns corresponding to retrieval of the excitations sequence synthesized in [36]: comparison amongst the ground truth (blue curve), the solution achieved by performing **only step (i)** of the proposed procedure (green curve), and the solution achieved by performing **steps (i) and (ii)** of the proposed procedure (red curve). SNR=25 dB.

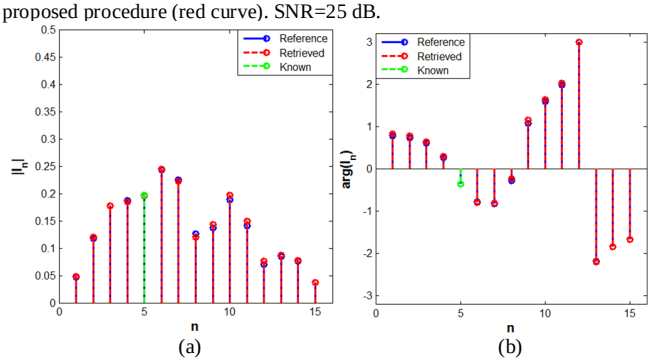

Fig. 10. Excitation amplitudes (a) and phases (b) concerning PR of the source synthesized in [36]: ground truth (blue curve), and solution achieved by performing **steps (i) and (ii)** of the proposed procedure (red curve). The a-priori known excitation is plotted in green color.

In the third test case, in order to validate the applicability of the proposed approach to cases where mutual-coupling and mounting-platform effects play a role, we exploited as reference the power pattern radiated by the antenna shown in Fig. 11, i.e., an array of 10 truncated rectangular metallic waveguides. These latter measure 10.37mm x 1.32mm and have been placed on a perfectly conductor plane (in order to avoid radiation effects behind the antenna) with a constant inter-element spacing equal to 7.52mm. The radiated field (whose directivity behavior is shown in Fig. 12) has been computed through a full-wave simulation by exploiting the CST Microwave Studio™ software at the usual *Ka* frequency for satellite communications, i.e., f=19.95GHz. In order to

This is the post-print of the following article: A. F. Morabito, R. Palmeri, V. A. Morabito, A. R. Laganà, and T. Isernia, "Single-Surface Phaseless Characterization of Antennas via Hierarchically Ordered Optimizations," IEEE Transactions on Antennas and Propagation, vol. 67, n. 1, pp. 461-474, 2019. Article has been published in final form at: https://ieeexplore.ieee.org/document/8502061. DOI: 10.1109/TAP.2018.2877270.

generate a general pencil beam, the reference excitations have been set as real and positive random variables (uniformly distributed in the interval [0,1]). Finally, in order to execute the PR procedure described in Section IV, the far field has been processed, by exploiting the guidelines in [31],[32], as the array factor of a 'virtual' equispaced array composed by 15 elements.

By performing step (i) of the procedure, we achieved NMSE=0.6679 and the power pattern shown in green color in Fig. 13. As in the previous test cases, execution of step (ii) of the procedure allowed achieving both a relevant improvement of performance (i.e., NMSE=0.0081) and a fully-satisfactory PR solution. The superposition of reference and retrieved solutions is shown in Fig. 13.

Notably, in all the above test cases there was no need to enter into step (iii) of the procedure. Such a circumstance can be attributed to the fact that many zeroes are present in the data, so that the reduction of the ambiguities induced by these zeroes (see the discussion above as well as [41]) and by the known excitation allows a fast retrieval. Hence, in order to enhance the difficulty of the problem, in the fourth and final 1-D test case we kept the array geometry exploited in the second example above and replaced the reference excitations with complex sequences whose real and imaginary parts are *random* variables uniformly distributed in the interval (-1,1). These excitations and the corresponding radiation pattern are shown in cyan color in figures 14 and 15, respectively. In this harder scenario, in order to achieve a satisfactory fitting between the reference and retrieved solutions (i.e., NMSE=0.06) it has been necessary to iterate the proposed procedure beyond step (iv) by considering the five data samples having the largest intensity. The retrieved excitations and the corresponding power pattern are shown in magenta color in figures 14 and 15, respectively. As it can be seen, despite the increased problem difficulty, the approach kept ensuring a high PR accuracy. These results support, on the one hand, the generality of the proposed technique (as it can be used on any reference signal) and, on the other hand, its higher performance in antenna synthesis and characterization. In fact, in these problems the reference signal corresponds to the source and, rather than being randomly set, is usually chosen in such a way to generate a pencil or a shaped beam and a good radiation efficiency [48] (which, in turn, implies many zeroes on the data).

The NMSE values achieved in all numerical simulations are summarized by the figure reported at the end of the Section. Besides the accuracy of the overall solution procedure, these results testify the actual capability of strongly reducing the number of actual optimizations required to achieve a satisfactory recovery of the ground truth. As expected, this reduction becomes more and more noticeable as the field's number of zeroes increases (which is indeed the case for the actual signals relative to antenna applications).

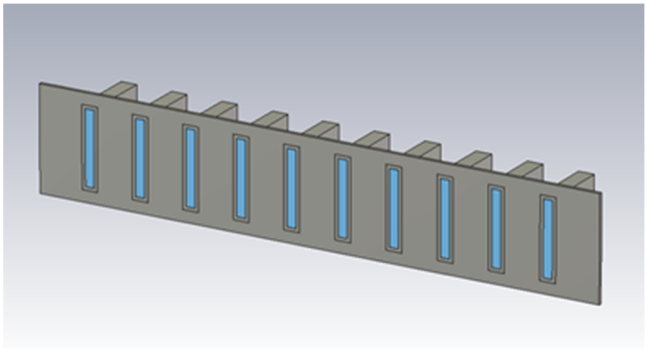

Fig. 11. External structure of the array of truncated waveguides exploited as source in the third test case of Section V.A.

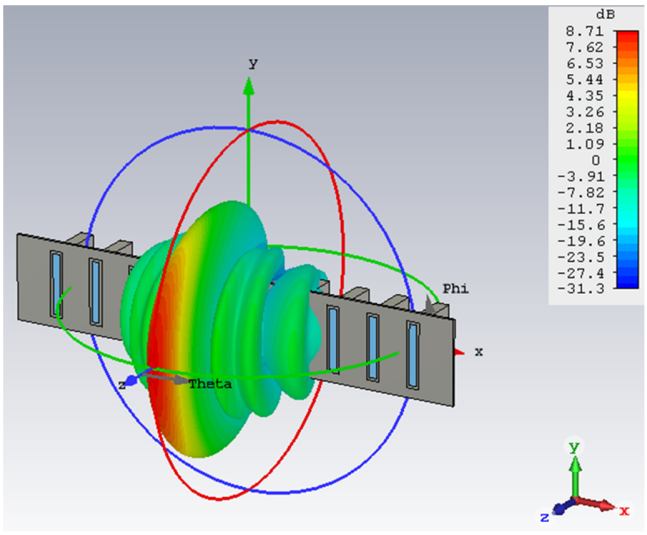

Fig. 12. Directivity pattern of the realistic array shown in Fig. 11 (CST™ full-wave simulation).

This is the post-print of the following article: A. F. Morabito, R. Palmeri, V. A. Morabito, A. R. Laganà, and T. Isernia, "Single-Surface Phaseless Characterization of Antennas via Hierarchically Ordered Optimizations," IEEE Transactions on Antennas and Propagation, vol. 67, n. 1, pp. 461-474, 2019. Article has been published in final form at: https://ieeexplore.ieee.org/document/8502061. DOI: 10.1109/TAP.2018.2877270.

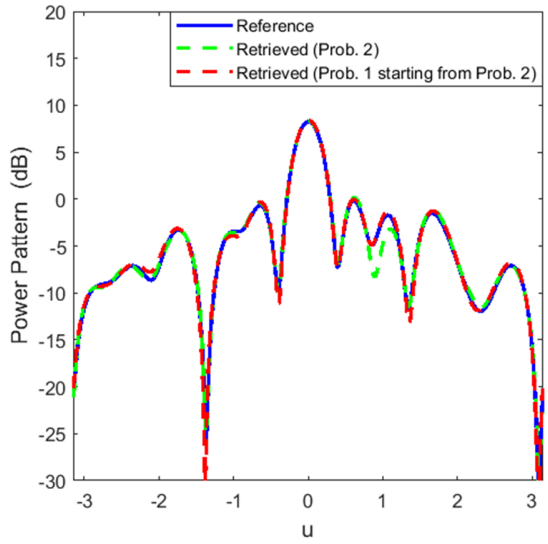

Fig. 13. Power patterns corresponding to the retrieval of the excitations of the realistic array shown in Fig. 11: ground truth (blue curve); solution achieved by performing **only step (i)** of the proposed procedure (green curve); solution achieved by performing **steps (i) and (ii)** of the proposed procedure (red curve). SNR=25 dB.

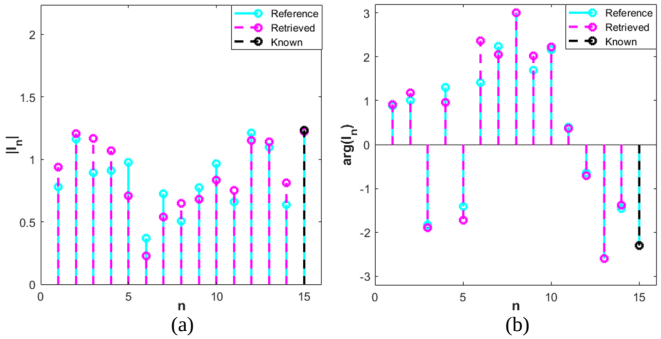

Fig. 14. Excitation amplitudes (a) and phases (b) concerning the retrieval of a complex random signal: comparison between the ground truth (cyan curve) and the achieved solution (magenta curve). The a-priori known excitation is depicted in black color.

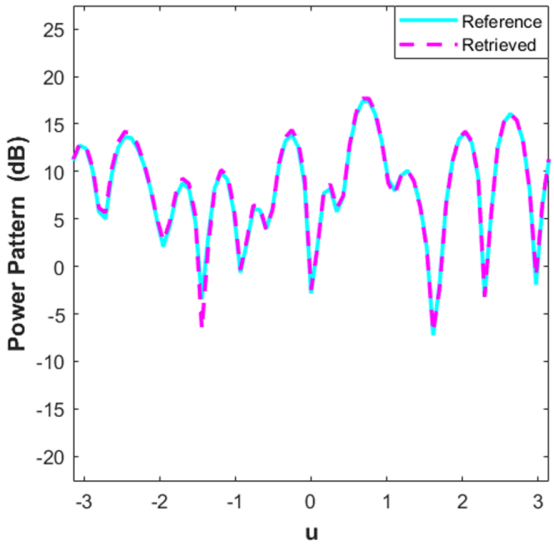

Fig. 15. Power patterns corresponding to retrieval of the random excitations shown in Fig. 14. SNR=25 dB.

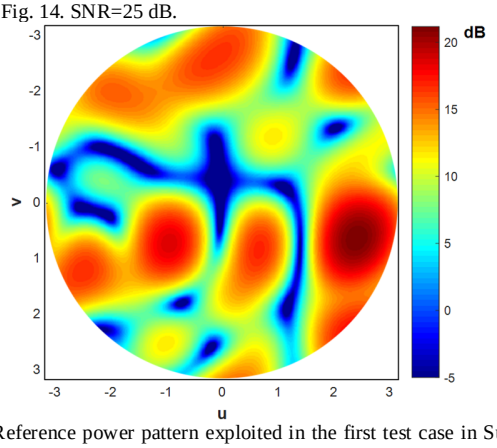

Fig. 16. Reference power pattern exploited in the first test case in Subsection V.B (25-elements square array, SNR=25 dB).

This is the post-print of the following article: A. F. Morabito, R. Palmeri, V. A. Morabito, A. R. Laganà, and T. Isernia, “Single-Surface Phaseless Characterization of Antennas via Hierarchically Ordered Optimizations,” IEEE Transactions on Antennas and Propagation, vol. 67, n. 1, pp. 461-474, 2019. Article has been published in final form at: https://ieeexplore.ieee.org/document/8502061. DOI: 10.1109/TAP.2018.2877270.

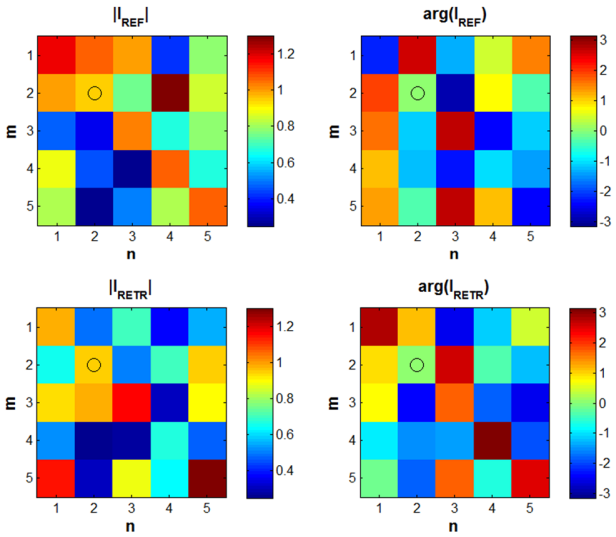

Fig. 17. Solution retrieved in the first test case of Subsection V.B by performing **only step (i)** of the procedure: reference (in the top) and retrieved (in the bottom) excitations. Amplitude and phase distributions are shown on the left and right sides, respectively. The a-priori known excitation is marked with a circle.

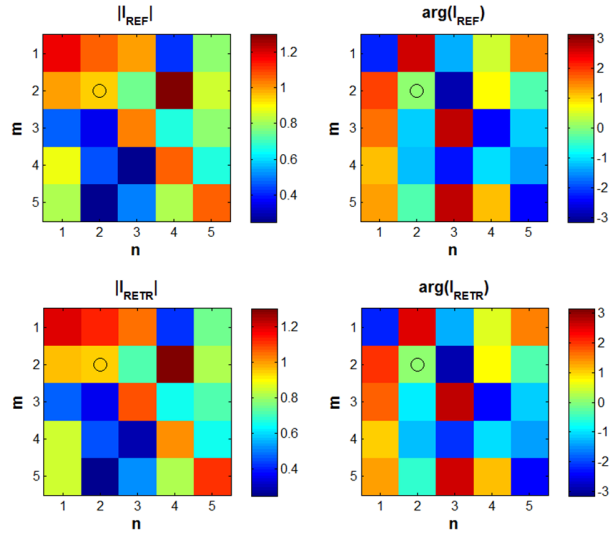

Fig. 18. Solution retrieved in the first test case of Subsection V.B by performing **steps (i) and (ii)** of the procedure: reference (in the top) and retrieved (in the bottom) excitations. Amplitude and phase distributions are shown on the left and right sides, respectively. The a-priori known excitation is marked with a circle.

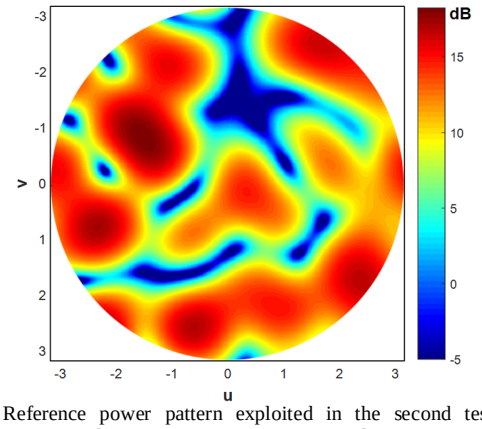

Fig. 19. Reference power pattern exploited in the second test case in Subsection V.B (25-elements square array, SNR=20 dB).

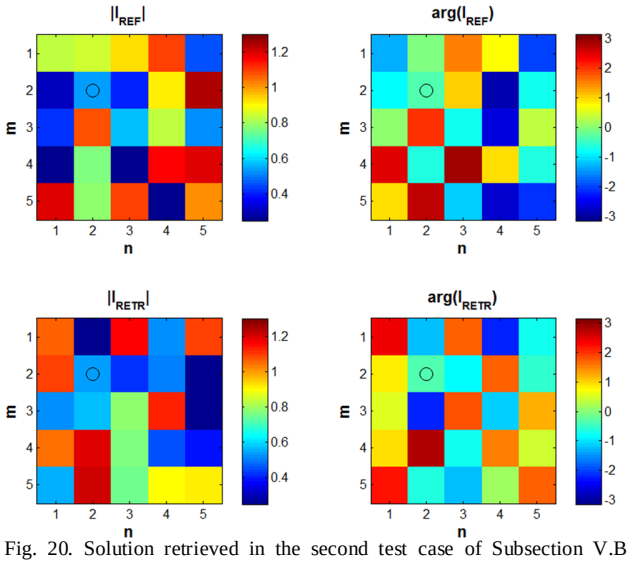

Fig. 20. Solution retrieved in the second test case of Subsection V.B by performing **steps (i) and (ii)** of the proposed procedure: reference (in the top) and retrieved (in the bottom) excitations. Amplitude and phase distributions are shown on the left and right sides, respectively. The a-priori known excitation is marked with a circle.

This is the post-print of the following article: A. F. Morabito, R. Palmeri, V. A. Morabito, A. R. Laganà, and T. Isernia, “Single-Surface Phaseless Characterization of Antennas via Hierarchically Ordered Optimizations,” IEEE Transactions on Antennas and Propagation, vol. 67, n. 1, pp. 461-474, 2019. Article has been published in final form at: https://ieeexplore.ieee.org/document/8502061. DOI: 10.1109/TAP.2018.2877270.

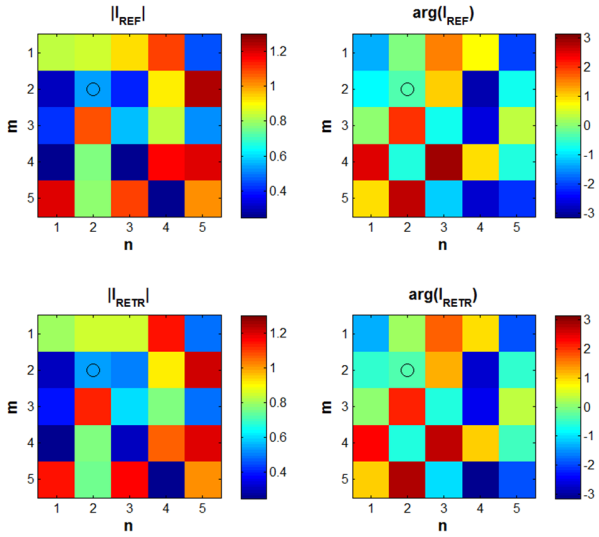

Fig. 21. Solution retrieved in the second test case of Subsection V.B by performing **steps i-iv** of the proposed procedure: reference (in the top) and retrieved (in the bottom) excitations. Amplitude and phase distributions are shown on the left and right sides, respectively. The a-priori known excitation is marked with a circle.

V.B Two-dimensional arrays

We present in this Subsection the outcomes achieved in the retrieval of 2-D arrays' excitations and fields. In particular, we deal with arrays radiating a field given by (10) with $Q=S$ and $d_x=d_y=\lambda/2$ (according to the rules given in Appendix I).

In order to test the method under severe conditions, we also consider herein random excitations[3]. In particular, the reference coefficients have been set as complex sequences whose real and imaginary parts are random variables uniformly distributed in the interval (-1,1).

As a first test case, an equispaced square array composed of 25 isotropic elements has been set as signal source and an SNR=25 dB has been adopted. The reference power pattern and excitations are respectively shown in figures 16 and 17.

By executing step (i) of the procedure, the excitations depicted in Fig. 17 have been achieved (NMSE=1.27). As a slight discrepancy between the results and the ground truth was present, step (ii) of the procedure has also been executed. By so doing, excitations shown in Fig. 18 have been retrieved, leading a much better fitting (NMSE=0.0166).

In order to test the approach in a harder scenario, we repeated the experiment by setting SNR=20 dB. The reference power pattern and excitations pertaining to this case are respectively shown in figures 19 and 20.

To carry out PR, we first performed steps (i) (leading to NMSE=2.0509) and (ii) (leading to NMSE=1.8483) of the procedure, which provided the solution shown in Fig. 20. As it can be seen, due to the lower SNR value, this time the execution of only these two steps did not suffice to achieve a good fitting between data and solution. However, it has been possible to successively solve the PR problem by performing just the two successive steps of the procedure. In particular, a fully-satisfactory fitting between data and solution has been achieved through the execution of steps (iii) (leading to NMSE=0.9498) and (iv) (leading to NMSE=0.0231). The retrieved excitations are shown in Fig. 21.

As final test case, we assessed the approach by setting the signal source as a much larger array. In particular, we considered a 100-elements square array and exploited as reference the random excitations depicted in Fig. 22. The corresponding power pattern, which has been corrupted by a noise such that SNR=25 dB, is shown in Fig. 23. Notably, by executing steps (i) (leading to NMSE=2.6544) and (ii) (leading to NMSE=0.0816), the excitations shown in Fig. 22 have been achieved. As it can be seen, despite the considerably-increased number of unknowns, the proposed technique kept providing a good fitting between data and solution.

The NMSE values achieved in all numerical simulations are summarized by Fig. 24. As in the 1-D cases, these results confirm the effectiveness of the proposed approach as well as its capability of achieving a fully-satisfactory solution by means of a small number of hierarchically-ordered optimizations.

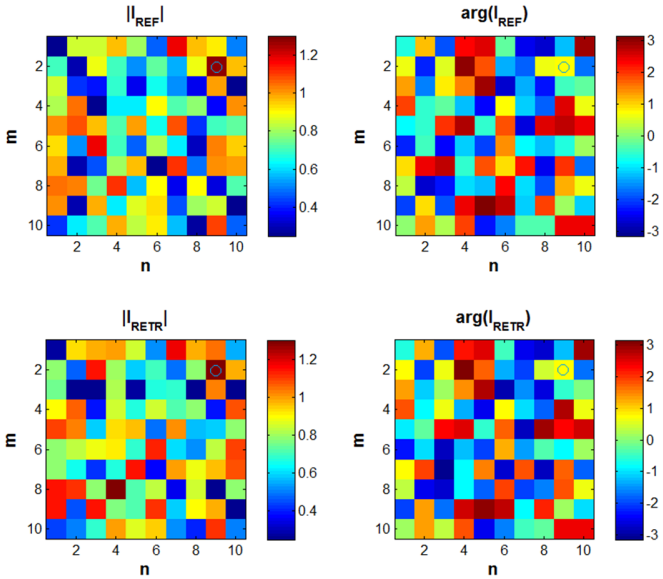

Fig. 22. Reference (in the top) and retrieved (in the bottom) excitations for the 100-elements array. Amplitude and phase distributions are shown on the left and the right, respectively. The known excitation is marked with a circle.

[3] Note that such a circumstance allows anyway not incurring into factorable fields where, at least in the case of *u-v* factorable patterns, more than one single information would be needed for theoretical uniqueness.

This is the post-print of the following article: A. F. Morabito, R. Palmeri, V. A. Morabito, A. R. Laganà, and T. Isernia, "Single-Surface Phaseless Characterization of Antennas via Hierarchically Ordered Optimizations," IEEE Transactions on Antennas and Propagation, vol. 67, n. 1, pp. 461-474, 2019. Article has been published in final form at: https://ieeexplore.ieee.org/document/8502061. DOI: 10.1109/TAP.2018.2877270.

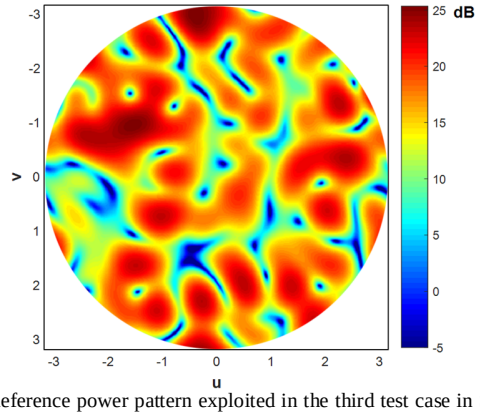

Fig. 23. Reference power pattern exploited in the third test case in Subsection V.B (100-elements square array, SNR=25 dB).

VI. Conclusions

A completely new point of view to the problem of determining the complex scalar field radiated by a finite-dimensional source starting from the knowledge of just its modulus, along with a corresponding solution procedure, has been proposed, discussed, and tested.

The problem has been formulated as the constrained maximization of a cost function related to the energy of the signal whose phase has to be retrieved. Then, by using a proper relaxation of the cost function as well as effective field representations, the overall problem has been reduced to a series of hierarchically-ordered optimizations. The introduced procedures can be used in a simple fashion in both cases of far-field and (by reasoning in terms of the so-called 'reduced radiated field' [33]) near-field measurements.

Numerical examples involving realistic noise levels and real-world array antennas confirmed the capabilities of the approach to recover the actual ground truth in a reliable fashion and with a limited computational burden starting from a single set of measurements and a minimal number of additional information.

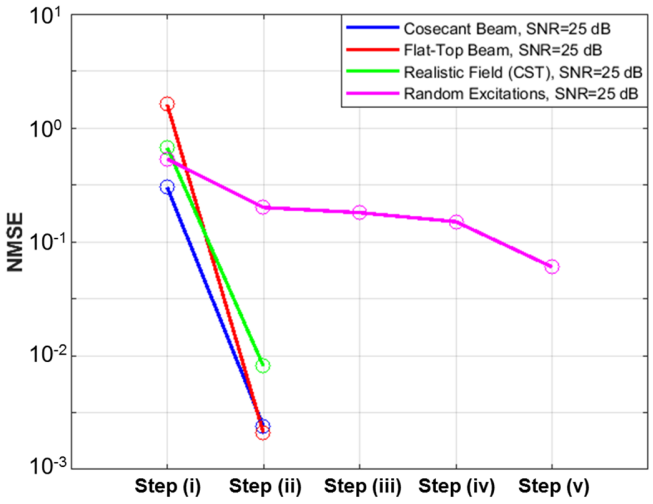

(a)

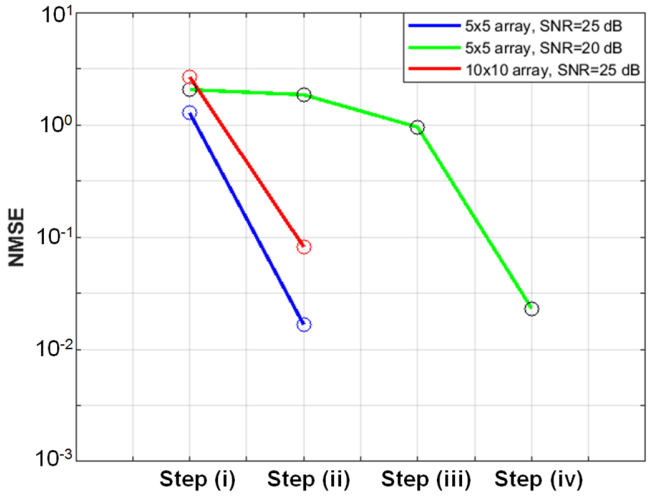

(b)

Fig. 24. NMSE achieved through the different steps of the proposed procedure: (a) test cases involving 1-D arrays; (b) test cases involving 2-D arrays.

Acknowledgment

The authors thank Space Engineering S.p.A. (Airbus Defence and Space) for having provided the data concerning the realistic antenna exploited in Section V.

Appendix I

The aim of this Appendix is that of providing some details concerning the measurement domain which is *actually* available when the far field can be expressed as in (2) or (10).

This is the post-print of the following article: A. F. Morabito, R. Palmeri, V. A. Morabito, A. R. Laganà, and T. Isernia, "Single-Surface Phaseless Characterization of Antennas via Hierarchically Ordered Optimizations," IEEE Transactions on Antennas and Propagation, vol. 67, n. 1, pp. 461-474, 2019. Article has been published in final form at: https://ieeexplore.ieee.org/document/8502061. DOI: 10.1109/TAP.2018.2877270.

Let us first consider the 1-D case relative to expression (2). In this scenario, differently from a generic PR problem wherein measurements can be taken over the whole domain of the function, measuring will be possible just over the *visible range*, i.e., $-\beta d \le u \le \beta d$. Therefore, since $AF(u)$ is a periodic trigonometric function (with periodicity range $-\pi \le u \le \pi$), one of the two following circumstances will come into play:

- if $d > \lambda/2$ then the visible space will be larger than the periodicity interval of the field (and hence it will suffice to pick power-pattern samples just in the range $-\pi \le u \le \pi$);
- if $d = \lambda/2$ then the visible space will exactly cover the whole periodicity interval of the field;
- if $d < \lambda/2$ then the signal domain will not be fully available to the measurement system [see Fig. 1(a)], enhancing the difficulty of the PR problem with respect to a conventional one.

Therefore, an inter-element spacing $d \le \lambda/2$ is preferable.

A very similar rule holds true also for 2-D arrays. To derive it, let us now turn on the 2-D scenario given by the field expression (10). In this case, supposing $Q=S=N$ and $d_x=d_y=d$ (which leads to a square array composed by N^2 elements), the visible space turns out to be a circle of radius βd centered in the origin of the spectral plane [see Fig. 1(b)]. Then, the actual value of d will bring into play one of the two following circumstances:

- if $d \ge 0.707\lambda$ then the visible space covers the whole periodicity range $\{(u,v): -\pi \le u \le \pi, -\pi \le v \le \pi\}$ of the field;
- if $d < 0.707\lambda$ then a portion of the signal to be retrieved will not be measurable [see Fig. 1(b)], enhancing the PR difficulty.

While in the first event the number of *independent* power-pattern measurements, say W, by virtue of the theory in [44] results equal to:

$$W = 4\frac{Nd}{\lambda/2}\frac{Nd}{\lambda/2} = 16N^2\left(\frac{d}{\lambda}\right)^2 \tag{12}$$

in the second event such number will decrease proportionally to the ratio between the sizes of the visible space and of the periodicity range, i.e.:

$$W = 4\frac{Nd}{\lambda/2}\frac{Nd}{\lambda/2}\frac{\pi(\beta d)^2}{4\pi^2} = 16N^2\pi\left(\frac{d}{\lambda}\right)^4 \tag{13}$$

Since W, as a necessary condition for *any* PR feasibility, must be equal to or larger than the overall number of unknowns, relation (13) allows identifying the minimum value of d, say d_{MIN}, such to enable the solution procedures (including the ones described in this Sections III and IV). In fact, by equating (13) to the actual number of unknowns, i.e., $2N^2$ (note one is looking for N^2 complex excitations), one achieves:

$$d_{MIN} = \frac{\lambda}{\sqrt[4]{8\pi}} \approx 0.9\frac{\lambda}{2} \tag{14}$$

REFERENCES

[1] C. Fienup and J. Dainty. "Phase retrieval and image reconstruction for astronomy," § 7 in *Image Recovery: Theory and Application*, pp. 231-275, Academic Press, 1987.

[2] R. P. Millane "Phase retrieval in crystallography and optics," *Journal of the Optical Society of America A*, vol. 7, n. 3, pp. 394-411, 1990.

[3] R. M. Von Bunau, H. Fukuda, and T. Terasawa, "Phase retrieval from defocused images and its applications in lithography," *Japanese Journal of Applied Physics*, vol. 36, part 1, n. 12B.

[4] A. Grjasnow, A. Wuttig, and R. Riesenberg, "Phase resolving microscopy by multi-plane diffraction detection," *Journal of Microscopy*, vol. 231, pt. 1, pp. 115–123, 2008.

[5] A. Descloux, K. S. Grußmayer, E. Bostan, T. Lukes, A. Bouwens, A. Sharipov, S. Geissbuehler, A. L. Mahul-Mellier, H. A. Lashuel, M. Leutenegger, and T. Lasser, "Combined multi-plane phase retrieval and super-resolution optical fluctuation imaging for 4D cell microscopy," *Nature Photonics*, vol. 12, pp. 165–172, 2018.

[6] L. Taylor, "The phase retrieval problem," *IEEE Transactions on Antennas and Propagation*, vol. 29, n. 2, pp. 386-391, 1981.

[7] O. M. Bucci, G. D'Elia, G. Leone, and R. Pierri, "Far-field pattern determination from the near-field amplitude on two surfaces," *IEEE Transactions on Antennas and Propagation*, vol. 38, n. 11, pp. 1772-1779, 1990.

[8] O. M. Bucci, G. D'Elia, and M. D. Migliore, "An effective near-field far-field transformation technique from truncated and inaccurate amplitude-only data," *IEEE Transactions on Antennas and Propagation*, vol. 47, n. 9, pp. 1377-1385, 1999.

[9] A. Capozzoli, C. Curcio, G. D'Elia, and A. Liseno, "Phaseless antenna characterization by effective aperture field and data representations," *IEEE Transactions on Antennas and Propagation*, vol. 57, n. 1, pp. 215-230, 2009.

[10] S. Costanzo, G. Di Massa, and M. D. Migliore, "A novel hybrid approach for far-field characterization from near-field amplitude-only measurements on arbitrary scanning surfaces," *IEEE Transactions on Antennas and Propagation*, vol. 53, n. 6, pp. 1866-1874, 2005.

[11] A. P. Anderson and S. Sali, "New possibilities for phaseless microwave diagnostics - Part I: Error reduction techniques," *IEE Proceedings H - Microwaves, Antennas and Propagation*, vol. 132, n. 5, pp. 291-298, 1985.

[12] D. Morris, "Phase retrieval in the radio holography of reflector antennas and radio telescopes," *IEEE Transactions on Antennas and Propagation*, vol. 33, n. 7, pp. 749-755, 1985.

[13] R. G. Yaccarino and Y. Rahamat-Samii, "Phaseless bi-polar near field measurements and diagnostics of array antennas," *IEEE Transactions on Antennas and Propagation*, vol. 47, n.3, pp.574-583, 1999.

[14] A. F. Morabito, R. Palmeri, and T. Isernia, "A compressive-sensing-inspired procedure for array antenna diagnostics by a small number of phaseless measurements," *IEEE Transactions on Antennas and Propagations*, vol. 64, n. 7, pp. 3260-3265, 2016.

[15] R. Pierri, G. D'Elia, and F. Soldovieri, "A two probes scanning phaseless near-field far-field transformation technique," *IEEE Transactions on Antennas and Propagation*, vol. 47, n. 5, pp. 792-802, 1999.

[16] F. Soldovieri, A. Liseno, G. D'Elia, and R. Pierri, "Global convergence of phase retrieval by quadratic approach," *IEEE Transactions on Antennas and Propagation*, vol. 53, n. 10, pp. 3135-3141, 2005.

[17] G. Junkin, "Planar near-field phase retrieval using GPUs for accurate THz far-field prediction," *IEEE Transactions on Antennas and Propagation*, vol. 61, n. 4, pp. 1763-1776, 2013.

[18] T. Isernia, G. Leone, and R. Pierri, "Radiation pattern evaluation from near-field intensities on planes," *IEEE Transactions on Antennas and Propagation*, vol. 44, n. 5, pp. 701-710, 1996.

This is the post-print of the following article: A. F. Morabito, R. Palmeri, V. A. Morabito, A. R. Laganà, and T. Isernia, "Single-Surface Phaseless Characterization of Antennas via Hierarchically Ordered Optimizations," IEEE Transactions on Antennas and Propagation, vol. 67, n. 1, pp. 461-474, 2019. Article has been published in final form at: https://ieeexplore.ieee.org/document/8502061. DOI: 10.1109/TAP.2018.2877270.

[19] K. Inan and R. E. Diaz, "On the uniqueness of the phase retrieval problem from far field amplitude-only data," *IEEE Transactions on Antennas and Propagation*, vol. 59, n. 3, pp. 1053-1057, 2011.
[20] J. I. Echeveste, M. Á. González de Aza, J. Rubio, and J. Zapata, "Near-optimal shaped-beam synthesis of real and coupled antenna arrays via 3-D-FEM and phase retrieval," *IEEE Transactions on Antennas and Propagation*, vol. 64, n. 6, pp. 2189-2196, 2016.
[21] T. Manabe, T. Nishibori, K. Mizukoshi, F. Otsubo, S. Ochiai, and H. Ohmine, "Measurement of the offset-Cassegrain antenna of JEM/SMILES using a near-field phase-retrieval method in the 640-GHz band," *IEEE Transactions on Antennas and Propagation*, vol. 60, n. 8, pp. 3971-3976, 2012.
[22] G. Hislop, L. Li, and A. Hellicar, "Phase retrieval for millimeter-and-submillimeter-wave imaging," *IEEE Transactions on Antennas and Propagation*, vol. 57, n. 1, pp. 286-290, 2009.
[23] B. Fuchs and L. Le Coq, "Excitation retrieval of microwave linear arrays from phaseless far-field data," *IEEE Transactions on Antennas and Propagation*, vol. 63, n. 2, pp. 748-754, 2015.
[24] J. Laviada, A. Arboleya-Arboleya, Y. Alvarez-Lopez, C. Garcia-Gonzalez, and F Las-Heras, "Phaseless synthetic aperture radar with efficient sampling for broadband near-field imaging: theory and validation," *IEEE Transactions on Antennas and Propagation*, vol. 63, n. 2, pp. 573-584, 2015.
[25] A. Arboleya, J. Laviada, J. Ala-Laurinaho, Y. Álvarez, F. Las-Heras, and A. V. Räisänen, "Phaseless characterization of broadband antennas," *IEEE Transactions on Antennas and Propagation*, vol. 64, n. 2, pp. 484-495, 2016.
[26] Y. Alvarez, F. Las-Heras, and M. R. Pino, "The sources reconstruction method for amplitude-only field measurements," *IEEE Transactions on Antennas and Propagation*, vol. 58, n. 8, pp. 2776-2781, 2010.
[27] O. M. Bucci, L. Crocco, M. D'Urso, and T. Isernia, "Inverse scattering from phaseless measurements of the total field on open lines," *Journal of the Optical Society of America A*, vol. 23, n. 10, pp. 2566-2577, 2006.
[28] F. Üstüner, E. Aydemir, E. Güleç, M. Ilarslan, M. Çelebi, and E. Demirel, "Antenna radiation pattern measurement using an unmanned aerial vehicle," *Proceedings of the 31st URSI General Assembly and Scientific Symposium*, Beijing, China, 16-23 Aug. 2014.
[29] X. Zhang, J. Liu, and B. He, "Magnetic-resonance-based electrical properties tomography: A review," *IEEE Reviews in Biomedical Engineering*, vol. 7, pp. 87-96, 2014.
[30] O. M. Bucci, T. Isernia, and A. F. Morabito, "Optimal synthesis of circularly symmetric shaped beams," *IEEE Transactions on Antennas and Propagation*, vol. 62, n. 4, pp. 1954-1964, 2014.
[31] O. M. Bucci, T. Isernia, and A. F. Morabito, "An effective deterministic procedure for the synthesis of shaped beams by means of uniform-amplitude linear sparse arrays," *IEEE Transactions on Antennas and Propagation*, vol. 61, n. 1, pp. 169-175, 2013.
[32] Y. Liu, X. Huang, K. D. Xu, Z. Song, S. Yang, Q. H. Liu, "Pattern synthesis of unequally spaced linear arrays including mutual coupling using iterative FFT via virtual active element pattern expansion," *IEEE Transactions on Antennas and Propagation*, vol. 65, n.8, pp. 3950-3958, 2017.
[33] O. M. Bucci and M. D'Urso, "Power pattern synthesis of given sources exploiting array methods," *Proceedings of the Second European Conference on Antennas and Propagation*, Edinburgh, UK, 11-16 November 2007.
[34] T. Isernia, G. Leone, and R. Pierri "Phase retrieval of radiated fields," *Inverse Problems*, vol. 11, n.1, pp 183-203, 1995.
[35] R. Barakat and G. Newsam, "Necessary conditions for a unique solution to two-dimensional phase recovery," *Journal of Mathematical Physics*, vol. 25, n. 11, pp. 3190-3193, 1984.
[36] T. Isernia, O. M. Bucci, and N. Fiorentino, "Shaped beam antenna synthesis problem: Feasibility criteria and new strategies," *Journal of Electromagnetic Waves and Applications*, vol. 12, 103-137, 1998.
[37] T. Isernia, F. Soldovieri, G. Leone, and R. Pierri, "On the local minima in phase reconstruction algorithms," *Radio Science*, vol. 31, n. 6, pp. 1887-1899, 1996.
[38] D. H. Wolpert and W. G. Macready, "No free lunch theorems for optimization," *IEEE Transactions on Evolutionary Computation*, vol. 1, n. 1, pp. 67–82, 1997.
[39] R. Barakat and G. Newsam, "Algorithms for reconstruction of partially known, band-limited Fourier-transform pairs from noisy data," *Journal of the Optical Society of America A*, vol. 2, n. 11, pp. 2027-2039, 1985.
[40] J. R. Fienup, "Phase retrieval algorithms: a comparison," *Applied Optics*, vol. 21, n. 15, pp. 2758-2769, 1982.
[41] T. Isernia, G. Leone, R. Pierri, and F. Soldovieri, "Role of support information and zero locations in phase retrieval by a quadratic approach," *Journal of the Optical Society of America A*, vol. 16, n. 7, pp. 1845-1856, 1999.
[42] E. J. Candes, T. Strohmer, and V. Voroninski, "Phaselift: exact and stable signal recovery from magnitude measurements via convex programming," *Communications on Pure and Applied Mathematics*, vol. 66, n. 8, pp. 1241-1274, 2013.
[43] A. R. Laganà, A. F. Morabito, and T. Isernia, "Phase retrieval by constrained power inflation and signum flipping," *Radio Science*, vol. 51, n. 12, pp. 1855-1863, 2016.
[44] O. M. Bucci, C. Gennarelli, and C. Savarese, "Representation of electromagnetic fields over arbitrary surfaces by a finite and nonredundant number of samples," *IEEE Transactions on Antennas and Propagation*, vol. 46, n. 3, pp. 351-359, 1998.
[45] T. Isernia and A. F. Morabito, "Mask-constrained power synthesis of linear arrays with even excitations," *IEEE Transactions on Antennas and Propagation*, vol. 64, n. 7, pp. 3212-3217, 2016.
[46] A. F. Morabito and P. G. Nicolaci, "Optimal synthesis of shaped beams through concentric ring isophoric sparse arrays," *IEEE Antennas and Wireless Propagation Letters*, vol. 16, pp. 979-982, 2017.
[47] M. R. Garey and D. S. Johnson, *Computers and Intractability: A Guide to the Theory of NP-Completeness*, W. H. Freeman, 1979.
[48] A. F. Morabito, "Synthesis of maximum-efficiency beam arrays via convex programming and compressive sensing," *IEEE Antennas and Wireless Propagation Letters*, vol. 16, pp. 2404-2407, 2017.
[49] B. Fuchs, "Application of convex relaxation to array synthesis problems," *IEEE Transactions on Antennas and Propagation*, vol. 62, n. 2, pp. 634-640, 2014.
[50] M. D. Migliore, "The minimum trace regularization approach in electromagnetics: Theory and perspectives," *Proceedings of the 2017 IEEE International Symposium on Antennas and Propagation & USNC/URSI National Radio Science Meeting*, pp. 423-424, San Diego, USA , 9-14 July 2017.
[51] P. Rocca, M. Benedetti, M. Donelli, D. Franceschini, and A. Massa, "Evolutionary optimization as applied to inverse scattering problems," *Inverse Problems*, vol. 25, no. 12, pp. 1-41, 2009.
[52] X. Jiang, S. Rajan, and X. Liu, "Wirtinger flow method with optimal stepsize for phase retrieval," *IEEE Signal Processing Letters*, vol. 23, n. 11, pp. 1627-1631, 2016.
[53] R. S. Elliot and G. J. Stern, "A new technique for shaped beam synthesis of equispaced arrays," *IEEE Transactions on Antennas and Propagation*, vol. AP-32, n. 10, pp. 1129-1133, 1984.
[54] J. M. Cid, J. A. Rodriguez, and F. J. Ares-Pena, "Shaped power patterns produced by equispaced linear arrays: optimized synthesis using orthogonal sin*Nx*/sin*x* beams," *Journal of Electromagnetic Waves and Applications*, vol. 13, n. 7, pp. 985-992, 1999.

This is the post-print of the following article: A. F. Morabito, R. Palmeri, V. A. Morabito, A. R. Laganà, and T. Isernia, "Single-Surface Phaseless Characterization of Antennas via Hierarchically Ordered Optimizations," IEEE Transactions on Antennas and Propagation, vol. 67, n. 1, pp. 461-474, 2019. Article has been published in final form at: https://ieeexplore.ieee.org/document/8502061. DOI: 10.1109/TAP.2018.2877270.